

## Lyman Continuum Leakers at $z > 3$ in the GOODS-S Field: Starburst or Not?

SHUAI RU ZHU (朱帅儒) <sup>1,2</sup> FANG-TING YUAN\* <sup>1</sup> CHUNYAN JIANG <sup>1</sup> ZHEN-YA ZHENG <sup>1,2</sup> AND RUQIU LIN <sup>1,2</sup>

<sup>1</sup>Shanghai Astronomical Observatory, Chinese Academy of Sciences, 80 Nandan Road, Shanghai 200030, People's Republic of China

<sup>2</sup>School of Astronomy and Space Sciences, University of Chinese Academy of Sciences, No. 19A Yuquan Road, Beijing 100049, People's Republic of China

### ABSTRACT

We investigate the star-forming properties of 23 Lyman Continuum (LyC) leakers at  $z > 3$  in the Great Observatories' Deep Survey-South (GOODS-S) field based on a systematic review of LyC observations from the literature. Using data from the Hubble Space Telescope (HST) and the James Webb Space Telescope (JWST), we construct the spectral energy distributions (SEDs) for these LyC leakers, covering the spectrum from rest-frame ultraviolet to near-infrared. Through the application of a unified modeling approach, we measure the ultraviolet slope ( $\beta$ ), star formation rate, and stellar mass for these LyC leakers in a consistent manner. These high-redshift LyC leakers demonstrate statistically blue UV-continuum slopes ( $\beta$ ), which is consistent with their high escape fraction of LyC photons. We find that these high-redshift LyC leakers span a wide range of specific star formation rate ( $\log(\text{sSFR}/\text{yr})$  from -8.6 to -6.7). Ten of these LyC leakers are located on the star formation main sequence, instead of all being in the starburst mode. The results indicate that intense bursts of star formation are not necessarily required for the leakage of LyC photons for galaxies at  $z > 3$ .

### 1. INTRODUCTION

The epoch of reionization (EoR) is the last major phase change of the Universe, which happens at the redshift range of  $6 \lesssim z \lesssim 10$  constrained by the Gunn-Peterson trough observed in QSO spectra (e.g., Fan et al. 2006) and the CMB observations (e.g., Planck Collaboration et al. 2016). During the EoR, most of the neutral hydrogen in the intergalactic medium (IGM) is ionized by Lyman continuum photons (i.e. LyC photons,  $\lambda < 912 \text{ \AA}$ ) emitted by certain sources in the early universe, such as quasars and young stars in star-forming galaxies (e.g., Finkelstein et al. 2012a; Robertson et al. 2013; Madau & Haardt 2015; Dayal et al. 2020). Recent studies have shown that quasars contribute only a small fraction of ionizing photons required by reionization (e.g., Shen et al. 2020; Jiang et al. 2022; Mat-suoka et al. 2023), leaving star-forming galaxies to be the most likely sources of LyC photons contributing to cosmic reionization (e.g., Finkelstein et al. 2019; Mason et al. 2019; Naidu et al. 2020).

Theoretically, the ionizing photon budget during the EoR requires an average escape fraction of LyC photons

from galaxies to be about 20% (e.g., Ouchi et al. 2009; Robertson et al. 2013, 2015). However, in observation, it is unlikely to detect the ionizing emission of galaxies in the EoR directly due to the increasing absorption of the IGM with redshift. Therefore, we have to rely on lower redshift galaxies with leaking LyC radiation to study the mechanisms that drive the escape of LyC photons from galaxies.

Low redshift analogs at  $z \lesssim 0.3$ , owing to the negligible IGM absorption and the high sensitivity of HST/Cosmic Origins Spectrograph (COS), have been widely studied in search of diagnostics closely related to LyC escape (e.g., Borthakur et al. 2014; Izotov et al. 2018a,b; Flury et al. 2022). However, the low-redshift LyC leakers have complicated selection functions, and their properties may evolve to be distinct from galaxies in the EoR (e.g., Naidu et al. 2022).

Direct detection of LyC emission becomes feasible only when redshift decreases to  $z \lesssim 4.5$ , making  $3 < z < 4.5$  the closest window to the EoR to study the mechanisms that drive the escape of LyC photons from galaxies.

Since the 2000s, many efforts have been made to search for LyC leakers at  $z > 3$  (e.g., Steidel et al. 2001; Shapley et al. 2006; Iwata et al. 2009; Steidel et al. 2018; Vanzella et al. 2018; Marques-Chaves et al. 2021, 2022). Till now, dozens of galaxies at  $z > 3$  have been iden-

Corresponding author: Fang-Ting Yuan

\*email: yuanft@shao.ac.cn

tified as LyC leakers, indicating that some galaxies can have high escape fractions ( $\gtrsim 20\%$ ) of LyC photons (e.g., Vanzella et al. 2012; Shapley et al. 2016; Vanzella et al. 2016; Yuan et al. 2021). On the other hand, stacking analyses of galaxies without LyC detections result in a relatively small escape fraction ( $\lesssim 5\%$ , e.g. Grazian et al. 2016; Wang et al. 2023). It may suggest the diversity of properties that are connected to the escape of ionizing photons. Therefore, it is necessary to find the properties of LyC leakers that are connected to the LyC leakage, and then examine whether these properties are consistent with those of star-forming galaxies in the EoR where the LyC emissions are not detectable.

Several studies find that the LyC leakers at  $z > 3$  have blue UV slope  $\beta$  and are starbursts (e.g., de Barros et al. 2016; Begley et al. 2022; Pahl et al. 2023), consistent with the results based on the low redshift LyC leakers (e.g., Chisholm et al. 2022; Flury et al. 2022). In contrast, some studies find no dependence of LyC leakage on the physical properties of galaxies (e.g., Saxena et al. 2022; Liu et al. 2023). A possible cause of the discrepancy is that these works are based on different samples and methods.

In this study, we focus on the LyC leakers in the GOODS South field (GOODS-S, Giavalisco et al. 2004) to take advantage of the rich data in this field. We attempt to include all LyC leakers at spectroscopic redshift  $z > 3$  detected in previous studies. We include *Ion1*, first reported by Vanzella et al. (2012, V12) as a LyC leaker at  $z = 3.797$  based on the detection in the U-band with VIMOS (Le Fèvre et al. 2003). The LyC emission has been further confirmed by Ji et al. (2020, J20) using the F410M band image observed with the Hubble Space Telescope (HST). *Ion2* ( $z = 3.212$ ) is another LyC leakers whose LyC emission has been detected in the VIMOS spectrum, image, and HST F336W band (Vanzella et al. 2015, 2016; de Barros et al. 2016, DB16). Using the data of the Hubble Deep UV Legacy Survey (HDUV, Oesch et al. 2018), Yuan et al. (2021, Y21) found a LyC leaker at  $z = 3.797$  (CDFS-6664), whose LyC emission has been detected in the HST F336W band. Rivera-Thorsen et al. (2022, RT22) carried out a bottom-up search using the UV images from the Ultraviolet Hubble Ultra Deep Field (UVUDF, Teplitz et al. 2013; Rafelski et al. 2015) and HDUV (Oesch et al. 2018). They identified two new LyC leakers at  $z > 3$ . Saxena et al. (2022, S22) reported 11 LyC leakers based on narrow band (Guaita et al. 2016) and VIMOS-U band images (Nonino et al. 2009). Gupta et al. (2024, G24) newly discovered a LyC leakers (z19863) using the HST F336W filter. Kerutt

et al. (2024, K24) identified 12 LyC leakers based on HDUV (Oesch et al. 2018).

In the above studies, different methods and parameters are employed, which makes it hard to make a fair comparison between different works. Here we collect the information on all these LyC leakers and fit their spectral energy distributions (SEDs) with a common set of models to obtain their physical properties systematically.

In this work, we use the multiwavelength data provided by 3D-HST catalog (Skelton et al. 2014) and include the newest released data from James Webb Space Telescope (JWST, Gardner et al. 2023) to extend the wavelength coverage to the rest-frame near-infrared (NIR). In the SED fitting, we include emission line models to alleviate the effect of strong emission lines on broadband fluxes (e.g., de Barros et al. 2014; Yuan et al. 2019). Also, different from many previous works, we treat the escape fraction  $f_{\text{esc}}$  as a free parameter in the SED fitting. A few recent studies have already taken  $f_{\text{esc}}$  as a free parameter in their analysis (e.g., Marques-Chaves et al. 2021, 2022; Yuan et al. 2021; Kerutt et al. 2024). The escape fraction of ionizing photons is related to the number of young stars and therefore can affect the shape of the SEDs and the estimation of the star-formation rates (SFRs) of galaxies (Zackrisson et al. 2013; Rivera-Thorsen et al. 2022).

We introduce the sample of LyC leakers in Section 2, and present the data and method used in our study in Section 3. In Section 4, we investigate the star-forming properties of the LyC leakers based on the results of SED fitting. Finally, we summarize the work in Section 5. We adopt a standard cosmology model with parameters  $\Omega_M = 0.3$ ,  $\Omega_\Lambda = 0.7$ ,  $H_0 = 70 \text{ km s}^{-1} \text{ Mpc}^{-1}$ . All magnitudes throughout this paper are given in the AB system.

## 2. A SAMPLE OF LYC LEAKERS AT $Z > 3$

We have collected a sample of LyC leakers in the GOODS-S field with spectroscopic redshifts at  $z > 3$  from seven works (J20; DB16; Y21; S22; RT22; G24; K24).

We remove F336W-1041 in RT22 and CDFS 18454 in S22 because their SEDs cannot be fitted well ( $\chi^2 > 5$ ) using their spectroscopic redshifts, which may be due to mismatched redshifts. We exclude another source, CDFS 13385 in S22 because it is likely to be a low-redshift contaminator according to RT22. Furthermore, we find that CDFS 12448 in S22, F336W-189 in RT22, and 3052076 in K24 are the same object. CDFS-6664 in Y21 and 122021111 in K24 are also the same object. The final sample contains 23 LyC leakers, as presented

in Table 1. These LyC leakers have an average redshift of about 3.505. Their redshifts range from 3.084 to 4.426.

We note that the LyC signals in this sample are detected in various bands with different signal-to-noise ratio (S/N) cuts. As listed in Table 1, eight LyC leakers are detected in the LyC band with an S/N larger than 3. All the galaxies in our sample have detections more than  $2\sigma$  in the LyC band. Among these LyC leakers, *Ion1*, *Ion2*, and F336W-189 are detected in two or more different bands. In Table 1, we summarize the basic information about the LyC signal of each source derived in previous works, including the bands in which the LyC signal was observed, the S/N of the LyC detection, and  $f_{\text{esc}}$  measurements. We also investigate the multiwavelength images of each object and record an offset if the separation between the centers of the LyC band and the nonionizing band is greater than  $0.1''$ .

For comparison, we also include three high-confidence LyC leakers in other fields, which are *Ion3* at  $z \sim 4$ , J0121+0025 at  $z \sim 3.244$ , and J1316-2614 at  $z \sim 3.6130$  (Vanzella et al. 2018; Marques-Chaves et al. 2021, 2022, 2024). No significant offset between the LyC and nonionizing UV emission is found in these LyC leakers. The methodologies applied in these works are consistent with ours, allowing us to use their results on the physical properties directly.

### 3. DATA AND METHOD

In the GOODS-S field, there are deep photometric observations of galaxies covering a wide range of wavelengths. All the sources in our sample have broadband flux measurements from HST, VLT/ISAAC, and *Spitzer*. 16 of 23 LyC leakers have been observed by JWST. The extensive photometric data allows us to perform more reliable SED fitting. By fitting these broadband fluxes in a consistent way, we can then study the physical properties of these galaxies systematically. We summarize the photometric data and the models we use in SED fitting, as well as those used in previous studies in Table 2.

#### 3.1. Photometric data

The broadband fluxes of these sources are taken from the 3D-HST catalog (Brammer et al. 2012; Skelton et al. 2014), which includes the measurements from HST, VLT/IASSC and *Spitzer* (specifically, the HST

F435W, F606W, F775W, F814W, F850LP, F125W, F140W, F160W bands; the VLT/IASSC  $K_s$  band; and the *Spitzer* IRAC1, IRAC2, IRAC3, IRAC4 bands). We use the total flux in the catalog introduced in Skelton et al. (2014).

We take the JWST photometry for the 16 LyC leakers covered by the JWST Advanced Deep Extragalactic Survey (JADES, Eisenstein et al. 2023), the First Reionization Epoch Spectroscopically Complete Observations (FRESCO, Oesch et al. 2023), and the JWST Extragalactic Medium-band Survey (JEMS, Williams et al. 2023). We use the total fluxes in the JADES data release 2 catalog for their JWST photometry (Rieke et al. 2023).

In the JADES catalog, CDFS 15718 is identified as two distinct objects, whereas it is listed as a single object in the 3D-HST catalog. In the SED fitting, we calculate the JWST flux for CDFS 15718 by summing the total fluxes of both counterparts.

#### 3.2. SED fitting

We use Code Investigating GALaxy Emission (CIGALE, Boquien et al. 2019) to derive the physical properties of these LyC leakers by fitting their broadband flux to the total model incorporating stars, gas, and dust. We note that CIGALE fitting is not suitable for the LyC bands because it takes an average IGM absorption (Meiksin 2006). We therefore exclude the LyC broadband flux (F225W, F275W, F336W) from the SED fitting.

We assume the Bruzual-Charlot Stellar Population Synthesis Models (BC03, Bruzual & Charlot 2003) and adopt the Chabrier initial mass function (IMF, Chabrier 2003). We note that using a different IMF (e.g., Salpeter Salpeter 1955) does not change our conclusion. The star formation history is modeled using a delayed form,  $SFR \propto t/\tau^2 \exp(t/\tau)$ , where  $t$  is the age from the onset of star formation and  $\tau$  is the characteristic time scale of star formation. The metallicity of stars is set to  $0.2Z_{\odot}$ , which is a typical value for high redshift galaxies (Finkelstein et al. 2012b).

For the stellar populations, we assume that the dust attenuation obeys the Calzetti Law (Calzetti et al. 2000), extended with the Leitherer et al. (2002) curve between the Lyman break and  $1500 \text{ \AA}$ , and the  $E(B-V)$  ranges from 0.001 to 0.15. For the nebular emission, we assume a Milky Way extinction curve (Cardelli et al. 1989). We assume that the nebular  $E(B-V)$  is equal to the stellar  $E(B-V)$  (e.g., Yuan et al. 2018; Buat et al. 2018).

CIGALE models the nebular emission based on the templates of Inoue et al. (2011), assuming that the nebular

**Table 1.** Sample of LyC leakers and basic properties.

Name <sup>a</sup>	R.A.	Decl.	Redshift	$f_{\text{esc}}^b$	LyC band	S/N <sub>LyC</sub>	Offset <sup>c</sup>	Reference
1181371 <sup>†</sup>	53.1358	-27.7955	3.084	$0.88 \pm 0.07$	F336W	$5.01\sigma$	Yes	K24
z19863 <sup>†</sup>	53.1699	-27.7684	3.088	$0.24 \pm 0.06$	F336W	$\sim 4\sigma$	Yes	G24
<i>Ion2</i> <sup>†</sup>	53.013515	-27.7552331	3.212	$0.25^{+0.004}_{-0.000}$	F336W (U, SpecVIMOS)	$\sim 10\sigma$	No	DB16
109004028 <sup>†</sup>	53.0994	-27.8392	3.267	$0.34 \pm 0.10$	F336W	$3.03\sigma$	Yes	K24
F336W-189 <sup>†</sup>	53.1679012	-27.7979524	3.46	$0.36 \pm 0.22$	F336W (U)	$\sim 3.6\sigma$	Yes	RT22
<i>Ion1</i> <sup>†</sup>	53.0693219	-27.7148184	3.794	$0.05 \pm 0.02$	U (F410M)	$\sim 10.3\sigma$	Yes	J20
<i>CDFS-6664</i> <sup>†</sup>	53.13885833	-27.83537861	3.797	$0.38 \pm 0.07$	F336W	$\sim 5\sigma$	Yes	Y21
126049137 <sup>†</sup>	53.2042	-27.8172	4.426	$0.69 \pm 0.10$	F336W	$4.39\sigma$	No	K24
CDFS 16444	53.1446546	-27.7711112	3.128	$0.30 \pm 0.07$	NB3727	$> 2\sigma$	No	S22
1521589	53.1283	-27.7887	3.152	$0.79 \pm 0.15$	F336W	$2.69\sigma$	Yes	K24
CDFS 24975	53.1457298	-27.6869713	3.187	$0.27 \pm 0.11$	NB3727	$> 2\sigma$	-	S22
CDFS 9358	53.1247187	-27.8245184	3.229	$0.14 \pm 0.07$	NB3727	$> 2\sigma$	-	S22
119004004	53.1891	-27.8363	3.314	$0.26 \pm 0.14$	F336W	$2.59\sigma$	No	K24
CDFS 5161	53.0545613	-27.862915	3.42	$0.53 \pm 0.24$	NB396	$> 2\sigma$	Yes	S22
CDFS 15718	53.1595397	-27.7767456	3.439	$0.28 \pm 0.10$	NB396	$> 2\sigma$	No	S22
CDFS 19872	53.1995306	-27.7414921	3.452	$0.29 \pm 0.30$	NB396	$> 2\sigma$	-	S22
CDFS 9692	53.0268389	-27.8209671	3.47	$0.38 \pm 0.19$	NB396	$> 2\sigma$	Yes	S22
CDFS 20745	53.0459052	-27.7336266	3.495	$0.38 \pm 0.30$	NB396	$> 2\sigma$	No	S22
3452147	53.1541	-27.7988	3.521	$0.47 \pm 0.14$	F336W	$2.60\sigma$	Yes	K24
4062373	53.1792	-27.7829	3.663	$0.74 \pm 0.13$	F336W	$2.21\sigma$	Yes	K24
4172404	53.1851	-27.7839	3.672	$0.31 \pm 0.15$	F336W	$2.88\sigma$	Yes	K24
5622786	53.1604	-27.8174	4.005	$0.53 \pm 0.11$	F336W	$2.05\sigma$	Yes	K24
122032127	53.1326	-27.8374	4.348	$0.77 \pm 0.14$	F336W	$2.33\sigma$	Yes	K24

<sup>†</sup> The high confidence sources.

<sup>a</sup> The ID of LyC leakers reported by S22 is from the CANDELS catalog (Guo et al. 2013). The ID of *CDFS-6664* is from the GOODS-MUSIC catalog (Grazian et al. 2006; Santini et al. 2009).

<sup>b</sup> The escape fraction of *Ion2* is determined using the relative escape fraction from DB16 and the E(B-V) values derived from SED fitting (see Section 3)

<sup>c</sup> An offset is noted if the separation between the centers of LyC band and the nonionizing band is greater than  $0''.1$ .

metallicity is equal to the stellar metallicity. The input parameters include the dimensionless ionization parameter  $U$  ( $U = q_{\text{ion}}/c$ , where  $q_{\text{ion}}$  is the ionization parameter) and the escape fraction of the LyC photons,  $f_{\text{esc}}$ . To compute the nebular emission spectrum, a normalized template of emission lines is selected based on the radiation field strength ( $U$ ) and metallicity ( $Z$ ). The spectrum is then rescaled to match the total ionizing photon luminosity for fitting. The ionizing photon luminosity is determined alongside the stellar population and corrected for the escape fraction of ionizing photons ( $f_{\text{esc}}$ ) using the following factor from Inoue et al. (2011):

$$k = \frac{1 - f_{\text{esc}} - f_{\text{dust}}}{1 + \alpha_B(T_e)/\alpha_B(T_e) \times (f_{\text{esc}} + f_{\text{dust}})}, \quad (1)$$

where  $\alpha_B$  is the case B recombination rate,  $\alpha_1$  is the recombination rate to the ground level,  $T_e$  the electron temperature in K. In the fitting, we take  $T_e = 10^4$  K. The corresponding  $\alpha_B$  and  $\alpha_1$  are set to be  $2.58 \times 10^{-19} \text{ m}^3 \text{ s}^{-1}$  and  $1.54 \times 10^{-19} \text{ m}^3 \text{ s}^{-1}$ , respectively (Ferland 1980, see also Boquien et al. 2019).  $f_{\text{dust}}$

is the partial absorption by dust before ionization. Here we assume that the dust affects only the nonionizing UV so that  $f_{\text{dust}}$  in the equation is 0 (see e.g., Steidel et al. 2018). We assume  $\log U = -2.5$  considering that this value corresponds to  $\log q_{\text{ion}}/\text{cm s}^{-1} = 8.0$ , which is consistent with the value for local LyC leakers (Nakajima & Ouchi 2014).

We compare the photometric data and the models used in our SED fitting with previous works in Table 2. Our SED fitting includes more photometric data to constrain the physical properties of the LyC leakers. Considering that the escape fraction of ionizing photons of these LyC leakers should be significantly larger than zero, it is more reasonable to set  $f_{\text{esc}}$  as a free parameter than to assume a zero escape fraction. Since we use a common set of photometric data and model assumptions for these LyC leakers the physical properties of these galaxies can be studied systematically.

The output parameters are estimated using a Bayesian approach. The parameters and the corresponding uncertainties are thus estimated from the probability distribu-



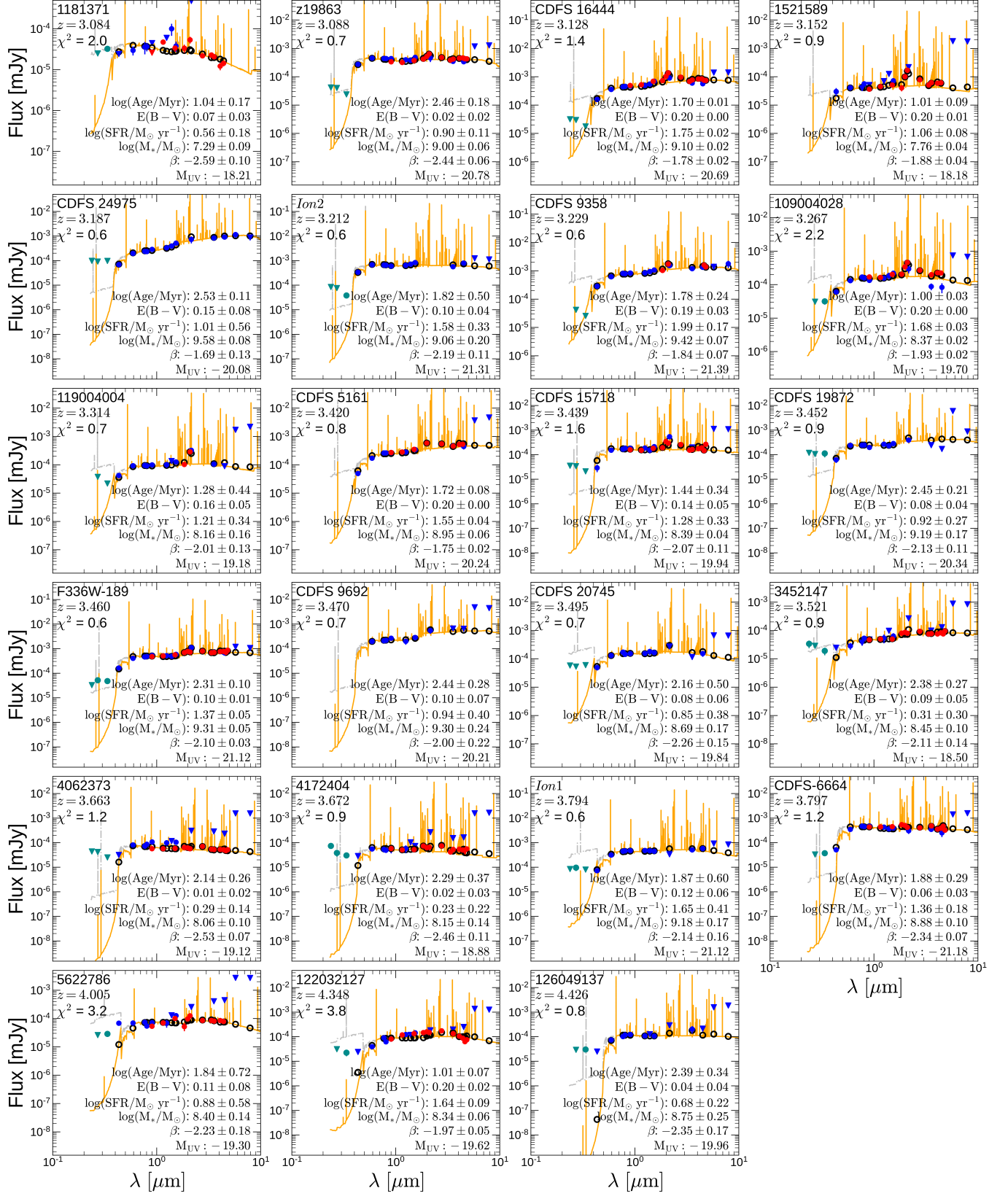


**Figure 1.** Observed SEDs (dots) of the LyC leakers. The red dots are measurements from the JADES catalog, and the blue and green dots are measurements from the 3D-HST catalog. The triangles indicate the  $3\sigma$  upper limits for non-detections. We exclude photometric points (in green) affected by the IGM. We show the best SED fit with orange solid lines (IGM attenuated) and grey dashed lines (IGM unattenuated). The integrated fluxes based on the best SED fit are shown in black circles.

**Table 2.** The photometric data and SED models

Refs.	Data	N <sub>phot</sub>	Wavelength range	IMF	SPS Model	SFH	Z (Z <sub>⊙</sub> )	Extinction curve	Nebular Model	f <sub>esc</sub>
S22	HST, Ks, <i>Spitzer</i>	14	0.4-8 μm	KB02	BC03	ExpDec	0-1	C00	F13	No
RT22	HST	11	0.2-1.5 μm	KB02	BC03	Delayed	0.2	C00	F17	No
Y21	HST, <i>Spitzer</i>	12	0.3-24 μm	Salpeter	BC03	Delayed	0.02-1	C00/CCM89	I10	Yes
DB16	HST, <i>Spitzer</i>	9	0.4-8 μm	Salpeter	BC03	Constant	0.2	S79	-	No
J20	HST, Ks, <i>Spitzer</i>	16	0.4-8 μm	K01	FSPS	Delayed	1	C00	F98,13	No
G24	HST, JWST	18	0.4-4.8 μm	Chabrier	BC03	Delayed	-	CF00	-	No
K24	HST, Ks, <i>Spitzer</i>	16	0.3-24 μm	Chabrier	BC03	Double exponential	0.005-1	C00/CCM89	I10	Yes
This work	HST, Ks, <i>Spitzer</i> , JWST	26	0.4-8 μm	Chabrier	BC03	Delayed	0.2	C00/CCM89	I10	Yes

NOTE—Column 1: Reference. Column 2: Photometric data sources. Column 3: Maximum number of photometric data points included in the SED fitting. Column 4: The wavelength range of photometric data. Column 5: Assumed stellar initial mass function. Column 6: Stellar population synthesis model used. Column 7: Assumed star formation history. Column 8: Assumed metallicity. Column 9: Assumed extinction curve. Column 10: Include nebular models in the SED fitting? (Yes/No) Column 11: Set ionizing photon escape fraction as a free parameter. (Yes/No)

Reference: [1] KB02: Kroupa & Boily (2002); [2] Salpeter: Salpeter (1955); [3] K01: Kroupa (2001); [4] FSPS: Conroy et al. (2009); [5] C00: Calzetti et al. (2000); [6] CCM89: Cardelli et al. (1989); [7] S89: Seaton (1979); [8] F13: Ferland et al. (2013); [9] F17: Ferland et al. (2017); [10] I10: Inoue (2010); [11] F98: Ferland et al. (1998); [12] F13: Ferland et al. (2013); [13] Chabrier: Chabrier (2003); [14] CF00: Charlot & Fall (2000)

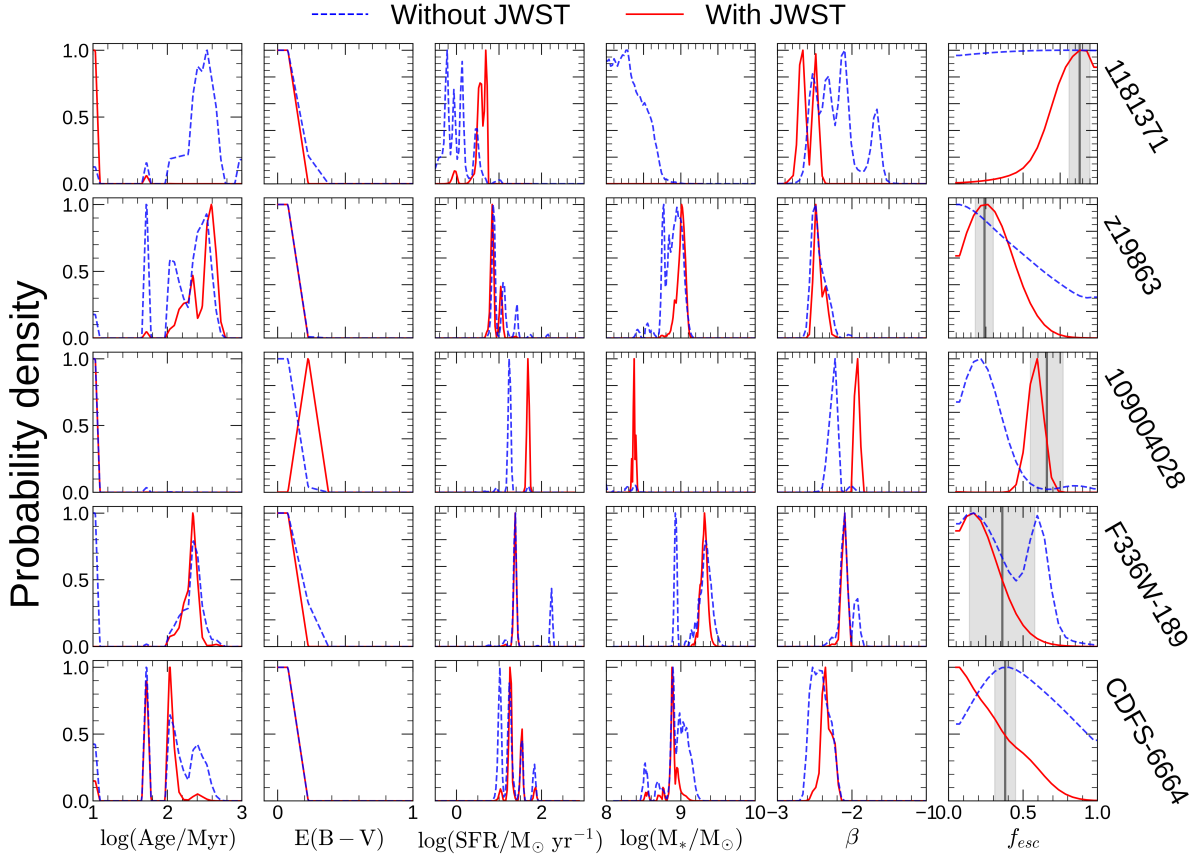


**Figure 2.** Probability density distributions for physical parameters (age, E(B-V), SFR,  $M_*$ ,  $\beta$ ) derived from SED fitting for 5 of the high confidence LyC leakers. The blue dashed lines are the probability distributions using 3D-HST photometric observations. The red solid lines are the probability distributions using 3D-HST photometric observations plus the observations of JWST. The use of the JWST photometric data provides better constraints on these star-forming parameters. In the last column, we also present the probability density distributions for  $f_{\text{esc}}$ . For reference, the  $f_{\text{esc}}$  values with their  $1\sigma$  errors reported in the literature are represented by the black lines and the grey areas.

tion function (PDF) by taking the likelihood-weighted mean and the standard deviation of all models. The goodness of the fit is estimated using the reduced  $\chi^2$  of the best model. Figure 1 shows the results of the SED fitting. 19 out of 23 LyC leakers in our sample have  $\chi^2 < 2.0$ .

For 15 of the 16 sources observed by JWST, more than four bands have been included in the SED fitting (see Figure 1), offering improved constraints on the physical parameters compared to those without the JWST bands, particularly for the stellar masses, as shown in Figure 2.

#### 4. RESULTS

In this section, we examine the star-forming properties of these LyC leakers. We focus on the  $\beta$ - $M_{\text{UV}}$  and  $\text{SFR}$ - $M_*$  relations of the high-redshift LyC leakers and compare them with the results derived from normal star-forming galaxies at a similar redshift. We present our results in Figure 3, where the color bar encodes  $f_{\text{esc}}$  of LyC leakers. We note that the  $f_{\text{esc}}$  calculated here strongly depends on the IGM models, and therefore has considerable uncertainties.

##### 4.1. $\beta$ - $M_{\text{UV}}$ relation

The UV-continuum spectrum slope  $\beta$  ( $f_\lambda \propto \lambda^\beta$ ) is an important parameter as it is sensitive to the metallicity, age, and especially the dust content within a galaxy. Since nebular continuum emission is significantly redder than the continuum emission from young and low-metallicity stars (e.g., [Leitherer & Heckman 1995](#)),  $\beta$  can also reflect the strength of nebular emission in a galaxy. Consequently,  $\beta$  can set constraints on the escape fraction of LyC photons (e.g., [Dunlop et al. 2013](#); [Zackrisson et al. 2013](#)).

We investigate the relation of  $\beta$  and  $M_{\text{UV}}$  of the  $z > 3$  LyC leakers in our sample (Figure 3a). The UV-continuum slope  $\beta$  is computed by fitting a straight line to the  $F_\lambda$  spectrum in log-log space over the wavelength ranges defined in Table 2 of [Calzetti et al. \(1994\)](#).  $M_{\text{UV}}$  is derived from the flux density at 1500 Å of the best-fit SED.

Figure 3a shows the UV-continuum slope  $\beta$  and  $M_{\text{UV}}$  for the high-redshift LyC leakers. The  $M_{\text{UV}}$  of the high-redshift sample ranges from -18.2 mag to -21.39 mag. The UV slope ranges from -2.6 to -1.7. We do not find a clear trend that the LyC leakers with lower UV luminosities have bluer UV slopes, as indicated in studies for high-redshift star-forming galaxies or low-redshift LyC leakers (e.g., [Bouwens et al. 2014](#); [Chisholm et al. 2022](#)). This may be partly due to the small size of the sample.

Most of the LyC leakers lie significantly below the mean relation at  $z \sim 4$  and show very blue  $\beta$

slopes, including seven galaxies in the GOODS-S (*Ion1*, *Ion2*, CDFS-6664, F336W-189, z19863, 1181371, and 126049137) which are either detected in more than one observation or with high signal-to-noise ratios ( $> 3$ ) and thus are the most reliable LyC leakers in our sample. The blue UV-continuum slopes of these galaxies suggest that these LyC leakers have young stellar populations, low metallicity, or low dust attenuation, consistent with the condition that allows LyC photons to leak.

Based on a sample of low-redshift ( $z \sim 0.3$ ) LyC leakers, [Chisholm et al. \(2022\)](#) find that the  $\beta$ - $M_{\text{UV}}$  relation for low-redshift LyC leakers is similar to that of  $z \sim 7$  galaxies predicted from [Bouwens et al. \(2014\)](#). Figure 3a shows that LyC leakers at  $z > 3$  statistically have bluer  $\beta$  slopes compared with  $z \sim 7$  LBGs or low-redshift LyC leakers. Given that the high-redshift LyC leakers in our sample have an average of  $f_{\text{esc}}=42\%$ , while the average  $f_{\text{esc}}$  of low-redshift LyC leakers is 8% (range from 0.4% to 58%), the observed bluer  $\beta$  is consistent with the correlation between  $\beta$  and  $f_{\text{esc}}$  as previously found by [Chisholm et al. \(2022\)](#).

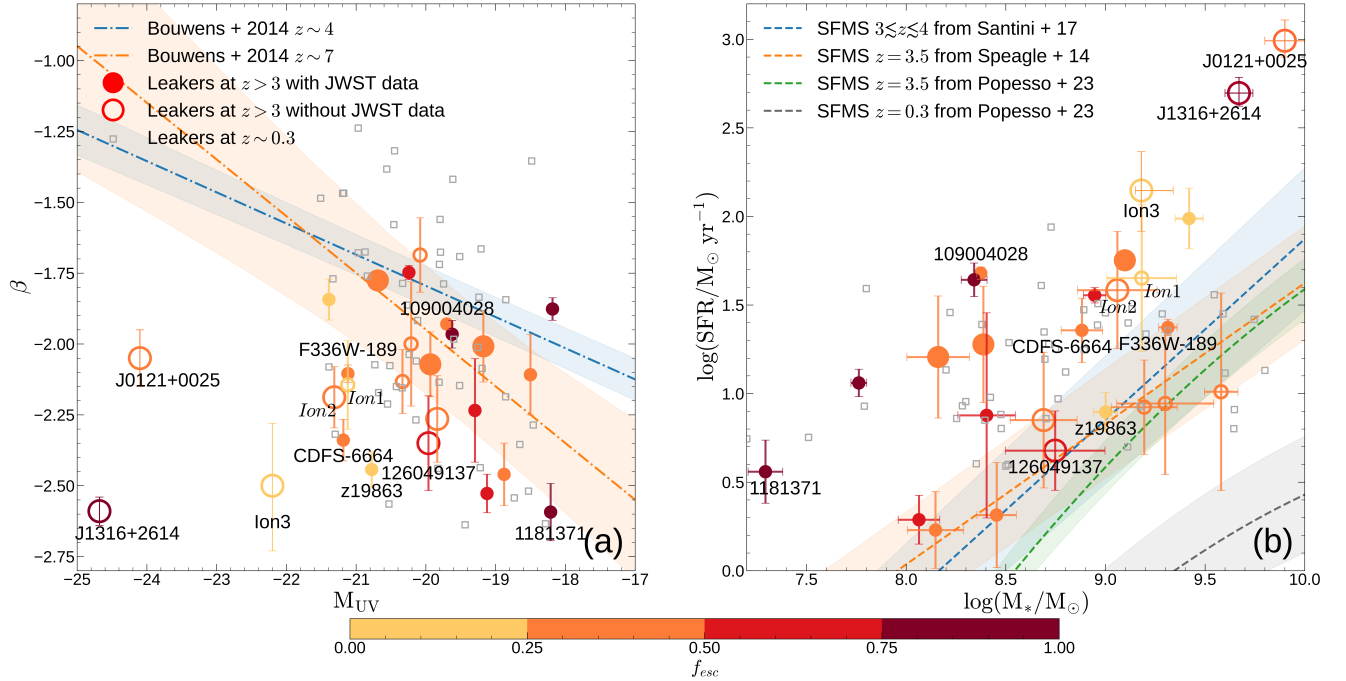
##### 4.2. $\text{SFR}$ - $M_*$ relation

Figure 3b shows the  $\text{SFR}$ - $M_*$  relation of the high-redshift LyC leakers in our sample. These high-redshift LyC leakers span a wide range of specific star formation rate ( $\log(\text{sSFR}/\text{yr})$  from -8.6 to -6.7). Using the star formation main sequence (SFMS) derived from [Speagle et al. \(2014\)](#), [Santini et al. \(2017\)](#), and [Popesso et al. \(2023\)](#) as the reference at  $z > 3$ , we find that 16 LyC leakers (including 3 LyC leakers not in GOODS-S) are distributed in the starburst region and the other 10 are on the SFMS.

The most vigorous starbursts in our sample, which have the highest specific SFR (sSFR) and are farthest above the main sequence lines in Figure 3b, show high escape fractions of LyC photons. Among them, four LyC leakers exhibit extremely high escape fractions ( $f_{\text{esc}} > 75\%$ ). However, we do not see a clear trend of  $f_{\text{esc}}$  as a function of sSFR. In fact, the average  $f_{\text{esc}}$  of LyC leakers on the SFMS and those in the starburst region are comparable.

Theoretically, vigorous starbursts generate a large number of ionizing photons and create density-bound HII regions or optical thin channels for the ionizing photons to escape. However, the fact that there are ten LyC leakers on the SFMS indicates that the extreme star formation may not be the fundamental reason that causes the escaping of ionizing photons.

The data suggests that starburst activity is not a prerequisite for high-redshift galaxies ( $z > 3$ ) to have a high escape fraction of ionizing photons. This finding con-



**Figure 3.** Star-forming properties of LyC leakers at  $z > 3$ . The filled and open circles indicate LyC leakers with and without JWST photometric data, respectively. Three LyC leakers at  $z > 3$  in other fields (Ion3, J0121+0025, J1316+2614) are also presented in this figure. The color indicates the  $f_{esc}$  of each LyC leaker. LyC leakers with offset (see Table 1) are indicated by small symbols. For comparison, we over plot a low- $z$  ( $z \sim 0.3$ ) sample of LyC leakers from Flury et al. (2022) as squares. (a) UV-continuum slope  $\beta$  as a function of UV absolute magnitude  $M_{UV}$ . The blue and orange lines show the  $\beta$ - $M_{UV}$  observed at  $z \sim 4$  and  $7$  from Bouwens et al. (2014), respectively. The shaded areas represent the 1- $\sigma$  dispersion of these relations. Most LyC leakers have bluer  $\beta$  than the star-forming galaxies at similar redshifts ( $z \sim 4$ ). Nine LyC leakers have extremely blue  $\beta$ , which are located even below the relation at  $z \sim 7$ . The  $z \sim 7$  relation is also applicable for low-redshift ( $z \sim 0.3$ ) LyC leakers as reported by Chisholm et al. (2022). (b) SFR as a function of stellar mass. The blue, orange, and green dashed lines indicate the star formation main sequence (SFMS) at  $z \sim 3.5$  derived from Santini et al. (2017), Speagle et al. (2014), and Popesso et al. (2023), respectively. The gray dashed line indicates the SFMS at  $z \sim 0.3$  derived from Popesso et al. (2023). Shaded areas represent the 1- $\sigma$  dispersion of these relations.

trasts with the characteristics of low-redshift LyC leakers in Flury et al. (2022). As shown in Figure 3b, all the low-redshift LyC leakers are identified as starbursts relative to the star-forming main sequence at  $z \sim 0.3$ . This distinction between high- and low-redshift LyC leakers may imply that different mechanisms are at play in the escape of LyC photons from these galaxies. Notably, LyC leakers at both  $z > 3$  and  $z \sim 0.3$  are positioned similarly on the SFR- $M_{*}$  plot, indicating a comparable level of star formation activity.

Some of our galaxies show offset between their LyC and nonionizing emission, which may indicate possible foreground contaminations (Nestor et al. 2013). In Figure 3, we use smaller symbols to distinguish sources with LyC offsets from those without. We find that LyC leakers with offset distribute similarly to those without offset. Therefore, including sources with offset LyC does not affect our conclusion.

We will explore more about the physical properties that are shared by LyC leakers. Especially, we find

that all of these high-redshift LyC leakers either show merging signatures or present an offset between the LyC emission and the optical emission which may suggest unresolved merger systems (Yuan et al. *in press*). The interaction may perturb the ISM in galaxies and produce channels with low optical depth for LyC photons to escape (Rauch et al. 2011; Gupta et al. 2024). We will study in more detail the morphology of LyC leakers in another work, to further investigate the driving mechanisms of the escape of the ionizing photons (Zhu et al., *in prep.*).

## 5. SUMMARY

We collect a sample of LyC leakers at  $z > 3$  in the GOODS-S field discovered by previous studies to investigate their physical properties systematically. We use a uniform set of photometric data and apply a common set of models and parameters in the SED fitting. We include the newest released JWST data in the analysis to give better constraints on the stellar mass and SFR. The



CIGALE code also allows us to include the nebular emission models and adjust the  $f_{\text{esc}}$  parameters to improve the quality of fitting for LyC leakers.

Analyzing the derived properties, we find that the UV-continuum slope  $\beta$  of high-redshift LyC leakers is statistically bluer than that of star-forming galaxies at the same redshift. Furthermore, the slope is bluer than low-redshift LyC leakers. The result is consistent with previous studies indicating a correlation between a bluer  $\beta$  and an increased  $f_{\text{esc}}$ .

Our analysis also reveals that 10 out of the 23 high-redshift LyC leakers do not fall into the starburst category. These 10 galaxies align with the properties of main sequence galaxies at similar redshifts. This result is in contrast to the findings for low-redshift ( $z \sim 0.3$ ) LyC leakers, which uniformly display significant starburst activity at  $z \sim 0.3$ .

Our results indicate that the intense bursts of star formation are not necessarily required for the LyC leakage at high redshift ( $z > 3$ ). In another work, we will further investigate the properties that may be related to the escape of LyC photons (Zhu et al. *in Prep.*).

Compared with previous works, we include more LyC leakers and estimate the properties in a consistent way. By integrating all the LyC leakers from previous works, we have obtained more information on the physical properties of LyC leakers. Our study is still limited by the small sample size of the high-redshift LyC leakers. The upcoming China Space Station Telescope (CSST, Zhan 2018) is equipped with the Multi-Channel Imager (MCI), which will carry out extremely deep observations in UV and optical bands with a spatial resolution comparable to HST and therefore will be able to detect more high-redshift LyC leakers. Furthermore, JWST will release more infrared data. With the aid of these future observations, we may further examine our conclusions using a larger sample with better data quality.

We thank the referee for providing helpful comments that have improved this work. This work is supported by the National Key R&D Program of China No.2022YFF0503402. It is partly supported by the Funds for Key Programs of Shanghai Astronomical Observatory. FTY acknowledges support from the Natural Science Foundation of Shanghai (Project Number: 21ZR1474300). ZYZ acknowledges support by the National Science Foundation of China (12022303), and the China-Chile Joint Research Fund (CCJRF No. 1906). We also acknowledge the science research grants from the China Manned Space Project, especially, NO. CMS-CSST-2021-A04, CMS-CSST-2021-A07.

This work is based on observations taken by the 3D-HST Treasury Program (GO 12177 and 12328) with the NASA/ESA HST, which is operated by the Association of Universities for Research in Astronomy, Inc., under NASA contract NAS5-26555.

This work is based on observations made with the NASA/ESA/CSA James Webb Space Telescope. The data were obtained from the Mikulski Archive for Space Telescopes at the Space Telescope Science Institute, which is operated by the Association of Universities for Research in Astronomy, Inc., under NASA contract NAS 5-03127 for JWST.

All the data used in this paper can be found in MAST: [10.17909/T9JW9Z](#) (Momcheva 2017), [10.17909/8tdj-8n28](#) (Rieke, Marcia et al. 2023) and [10.17909/fsc4-dt61](#) (Williams, Christina et al. 2023).

*Facilities:* HST (ACS, WFC3), VLT (IASSC), Spitzer (IRAC), JWST (NIRCam)

*Software:* Astropy (Astropy Collaboration et al. 2013, 2018, 2022), CIGALE (Boquien et al. 2019), Numpy (Harris et al. 2020), Matplotlib (Hunter 2007)

## REFERENCES

- Astropy Collaboration, Robitaille, T. P., Tollerud, E. J., et al. 2013, *A&A*, 558, A33, doi: [10.1051/0004-6361/201322068](https://doi.org/10.1051/0004-6361/201322068)
- Astropy Collaboration, Price-Whelan, A. M., Sipőcz, B. M., et al. 2018, *AJ*, 156, 123, doi: [10.3847/1538-3881/aabc4f](https://doi.org/10.3847/1538-3881/aabc4f)
- Astropy Collaboration, Price-Whelan, A. M., Lim, P. L., et al. 2022, *ApJ*, 935, 167, doi: [10.3847/1538-4357/ac7c74](https://doi.org/10.3847/1538-4357/ac7c74)
- Begley, R., Cullen, F., McLure, R. J., et al. 2022, *MNRAS*, 513, 3510, doi: [10.1093/mnras/stac1067](https://doi.org/10.1093/mnras/stac1067)
- Boquien, M., Burgarella, D., Roehlly, Y., et al. 2019, *A&A*, 622, A103, doi: [10.1051/0004-6361/201834156](https://doi.org/10.1051/0004-6361/201834156)
- Borthakur, S., Heckman, T. M., Leitherer, C., & Overzier, R. A. 2014, *Science*, 346, 216, doi: [10.1126/science.1254214](https://doi.org/10.1126/science.1254214)
- Bouwens, R. J., Illingworth, G. D., Oesch, P. A., et al. 2014, *ApJ*, 793, 115, doi: [10.1088/0004-637X/793/2/115](https://doi.org/10.1088/0004-637X/793/2/115)
- Brammer, G. B., van Dokkum, P. G., Franx, M., et al. 2012, *ApJS*, 200, 13, doi: [10.1088/0067-0049/200/2/13](https://doi.org/10.1088/0067-0049/200/2/13)
- Bruzual, G., & Charlot, S. 2003, *MNRAS*, 344, 1000, doi: [10.1046/j.1365-8711.2003.06897.x](https://doi.org/10.1046/j.1365-8711.2003.06897.x)
- Buat, V., Boquien, M., Małek, K., et al. 2018, *A&A*, 619, A135, doi: [10.1051/0004-6361/201833841](https://doi.org/10.1051/0004-6361/201833841)
- Calzetti, D., Armus, L., Bohlin, R. C., et al. 2000, *ApJ*, 533, 682, doi: [10.1086/308692](https://doi.org/10.1086/308692)
- Calzetti, D., Kinney, A. L., & Storchi-Bergmann, T. 1994, *ApJ*, 429, 582, doi: [10.1086/174346](https://doi.org/10.1086/174346)
- Cardelli, J. A., Clayton, G. C., & Mathis, J. S. 1989, *ApJ*, 345, 245, doi: [10.1086/167900](https://doi.org/10.1086/167900)
- Chabrier, G. 2003, *PASP*, 115, 763, doi: [10.1086/376392](https://doi.org/10.1086/376392)
- Charlot, S., & Fall, S. M. 2000, *ApJ*, 539, 718, doi: [10.1086/309250](https://doi.org/10.1086/309250)
- Chisholm, J., Saldana-Lopez, A., Flury, S., et al. 2022, *MNRAS*, 517, 5104, doi: [10.1093/mnras/stac2874](https://doi.org/10.1093/mnras/stac2874)
- Conroy, C., Gunn, J. E., & White, M. 2009, *ApJ*, 699, 486, doi: [10.1088/0004-637X/699/1/486](https://doi.org/10.1088/0004-637X/699/1/486)
- Dayal, P., Volonteri, M., Choudhury, T. R., et al. 2020, *MNRAS*, 495, 3065, doi: [10.1093/mnras/staa1138](https://doi.org/10.1093/mnras/staa1138)
- de Barros, S., Schaerer, D., & Stark, D. P. 2014, *A&A*, 563, A81, doi: [10.1051/0004-6361/201220026](https://doi.org/10.1051/0004-6361/201220026)
- de Barros, S., Vanzella, E., Amorín, R., et al. 2016, *A&A*, 585, A51, doi: [10.1051/0004-6361/201527046](https://doi.org/10.1051/0004-6361/201527046)
- Dunlop, J. S., Rogers, A. B., McLure, R. J., et al. 2013, *MNRAS*, 432, 3520, doi: [10.1093/mnras/stt702](https://doi.org/10.1093/mnras/stt702)
- Eisenstein, D. J., Willott, C., Albers, S., et al. 2023, arXiv e-prints, arXiv:2306.02465, doi: [10.48550/arXiv.2306.02465](https://doi.org/10.48550/arXiv.2306.02465)
- Fan, X., Strauss, M. A., Becker, R. H., et al. 2006, *AJ*, 132, 117, doi: [10.1086/504836](https://doi.org/10.1086/504836)
- Ferland, G. J. 1980, *PASP*, 92, 596, doi: [10.1086/130718](https://doi.org/10.1086/130718)
- Ferland, G. J., Korista, K. T., Verner, D. A., et al. 1998, *PASP*, 110, 761, doi: [10.1086/316190](https://doi.org/10.1086/316190)
- Ferland, G. J., Porter, R. L., van Hoof, P. A. M., et al. 2013, *RMxAA*, 49, 137, doi: [10.48550/arXiv.1302.4485](https://doi.org/10.48550/arXiv.1302.4485)
- Ferland, G. J., Chatzikos, M., Guzmán, F., et al. 2017, *RMxAA*, 53, 385, doi: [10.48550/arXiv.1705.10877](https://doi.org/10.48550/arXiv.1705.10877)
- Finkelstein, S. L., Papovich, C., Ryan, R. E., et al. 2012a, *ApJ*, 758, 93, doi: [10.1088/0004-637X/758/2/93](https://doi.org/10.1088/0004-637X/758/2/93)
- Finkelstein, S. L., Papovich, C., Salmon, B., et al. 2012b, *ApJ*, 756, 164, doi: [10.1088/0004-637X/756/2/164](https://doi.org/10.1088/0004-637X/756/2/164)
- Finkelstein, S. L., D'Aloisio, A., Paardekoooper, J.-P., et al. 2019, *ApJ*, 879, 36, doi: [10.3847/1538-4357/ab1ea8](https://doi.org/10.3847/1538-4357/ab1ea8)
- Flury, S. R., Jaskot, A. E., Ferguson, H. C., et al. 2022, *ApJS*, 260, 1, doi: [10.3847/1538-4365/ac5331](https://doi.org/10.3847/1538-4365/ac5331)
- Gardner, J. P., Mather, J. C., Abbott, R., et al. 2023, *PASP*, 135, 068001, doi: [10.1088/1538-3873/acd1b5](https://doi.org/10.1088/1538-3873/acd1b5)
- Giavalisco, M., Ferguson, H. C., Koekemoer, A. M., et al. 2004, *ApJL*, 600, L93, doi: [10.1086/379232](https://doi.org/10.1086/379232)
- Grazian, A., Fontana, A., de Santis, C., et al. 2006, *A&A*, 449, 951, doi: [10.1051/0004-6361:20053979](https://doi.org/10.1051/0004-6361:20053979)
- Grazian, A., Giallongo, E., Gerbasi, R., et al. 2016, *A&A*, 585, A48, doi: [10.1051/0004-6361/201526396](https://doi.org/10.1051/0004-6361/201526396)
- Guaita, L., Pentericci, L., Grazian, A., et al. 2016, *A&A*, 587, A133, doi: [10.1051/0004-6361/201527597](https://doi.org/10.1051/0004-6361/201527597)
- Guo, Y., Ferguson, H. C., Giavalisco, M., et al. 2013, *ApJS*, 207, 24, doi: [10.1088/0067-0049/207/2/24](https://doi.org/10.1088/0067-0049/207/2/24)
- Gupta, A., Trott, C. M., Jaiswar, R., et al. 2024, arXiv e-prints, arXiv:2403.13285, doi: [10.48550/arXiv.2403.13285](https://doi.org/10.48550/arXiv.2403.13285)
- Harris, C. R., Millman, K. J., van der Walt, S. J., et al. 2020, *Nature*, 585, 357, doi: [10.1038/s41586-020-2649-2](https://doi.org/10.1038/s41586-020-2649-2)
- Hunter, J. D. 2007, *Computing in Science & Engineering*, 9, 90, doi: [10.1109/MCSE.2007.55](https://doi.org/10.1109/MCSE.2007.55)
- Inoue, A. K. 2010, *MNRAS*, 401, 1325, doi: [10.1111/j.1365-2966.2009.15730.x](https://doi.org/10.1111/j.1365-2966.2009.15730.x)
- Inoue, A. K., Kousai, K., Iwata, I., et al. 2011, *MNRAS*, 411, 2336, doi: [10.1111/j.1365-2966.2010.17851.x](https://doi.org/10.1111/j.1365-2966.2010.17851.x)
- Iwata, I., Inoue, A. K., Matsuda, Y., et al. 2009, *ApJ*, 692, 1287, doi: [10.1088/0004-637X/692/2/1287](https://doi.org/10.1088/0004-637X/692/2/1287)
- Izotov, Y. I., Schaerer, D., Worseck, G., et al. 2018a, *MNRAS*, 474, 4514, doi: [10.1093/mnras/stx3115](https://doi.org/10.1093/mnras/stx3115)
- Izotov, Y. I., Worseck, G., Schaerer, D., et al. 2018b, *MNRAS*, 478, 4851, doi: [10.1093/mnras/sty1378](https://doi.org/10.1093/mnras/sty1378)
- Ji, Z., Giavalisco, M., Vanzella, E., et al. 2020, *ApJ*, 888, 109, doi: [10.3847/1538-4357/ab5fdc](https://doi.org/10.3847/1538-4357/ab5fdc)
- Jiang, L., Ning, Y., Fan, X., et al. 2022, *Nature Astronomy*, 6, 850, doi: [10.1038/s41550-022-01708-w](https://doi.org/10.1038/s41550-022-01708-w)
- Kerutt, J., Oesch, P. A., Wisotzki, L., et al. 2024, *A&A*, 684, A42, doi: [10.1051/0004-6361/202346656](https://doi.org/10.1051/0004-6361/202346656)

- Kroupa, P. 2001, *MNRAS*, 322, 231,  
doi: [10.1046/j.1365-8711.2001.04022.x](https://doi.org/10.1046/j.1365-8711.2001.04022.x)
- Kroupa, P., & Boily, C. M. 2002, *MNRAS*, 336, 1188,  
doi: [10.1046/j.1365-8711.2002.05848.x](https://doi.org/10.1046/j.1365-8711.2002.05848.x)
- Le Fèvre, O., Saisse, M., Mancini, D., et al. 2003, in *Society of Photo-Optical Instrumentation Engineers (SPIE) Conference Series*, Vol. 4841, Instrument Design and Performance for Optical/Infrared Ground-based Telescopes, ed. M. Iye & A. F. M. Moorwood, 1670–1681,  
doi: [10.1117/12.460959](https://doi.org/10.1117/12.460959)
- Leitherer, C., & Heckman, T. M. 1995, *ApJS*, 96, 9,  
doi: [10.1086/192112](https://doi.org/10.1086/192112)
- Leitherer, C., Li, I. H., Calzetti, D., & Heckman, T. M. 2002, *ApJS*, 140, 303, doi: [10.1086/342486](https://doi.org/10.1086/342486)
- Liu, Y., Jiang, L., Windhorst, R. A., Guo, Y., & Zheng, Z.-Y. 2023, *ApJ*, 958, 22, doi: [10.3847/1538-4357/acf9fa](https://doi.org/10.3847/1538-4357/acf9fa)
- Madau, P., & Haardt, F. 2015, *ApJL*, 813, L8,  
doi: [10.1088/2041-8205/813/1/L8](https://doi.org/10.1088/2041-8205/813/1/L8)
- Marques-Chaves, R., Schaerer, D., Álvarez-Márquez, J., et al. 2021, *MNRAS*, 507, 524,  
doi: [10.1093/mnras/stab2187](https://doi.org/10.1093/mnras/stab2187)
- . 2022, *MNRAS*, 517, 2972, doi: [10.1093/mnras/stac2893](https://doi.org/10.1093/mnras/stac2893)
- Marques-Chaves, R., Schaerer, D., Vanzella, E., et al. 2024, *arXiv e-prints*, arXiv:2407.18804,  
doi: [10.48550/arXiv.2407.18804](https://doi.org/10.48550/arXiv.2407.18804)
- Mason, C. A., Naidu, R. P., Tacchella, S., & Leja, J. 2019, *MNRAS*, 489, 2669, doi: [10.1093/mnras/stz2291](https://doi.org/10.1093/mnras/stz2291)
- Matsuoka, Y., Onoue, M., Iwasawa, K., et al. 2023, *ApJL*, 949, L42, doi: [10.3847/2041-8213/acd69f](https://doi.org/10.3847/2041-8213/acd69f)
- Meiksin, A. 2006, *MNRAS*, 365, 807,  
doi: [10.1111/j.1365-2966.2005.09756.x](https://doi.org/10.1111/j.1365-2966.2005.09756.x)
- Momcheva, I. 2017, 3D-HST, STScI/MAST,  
doi: [10.17909/T9JW9Z](https://doi.org/10.17909/T9JW9Z)
- Naidu, R. P., Tacchella, S., Mason, C. A., et al. 2020, *ApJ*, 892, 109, doi: [10.3847/1538-4357/ab7cc9](https://doi.org/10.3847/1538-4357/ab7cc9)
- Naidu, R. P., Matthee, J., Oesch, P. A., et al. 2022, *MNRAS*, 510, 4582, doi: [10.1093/mnras/stab3601](https://doi.org/10.1093/mnras/stab3601)
- Nakajima, K., & Ouchi, M. 2014, *MNRAS*, 442, 900,  
doi: [10.1093/mnras/stu902](https://doi.org/10.1093/mnras/stu902)
- Nestor, D. B., Shapley, A. E., Kornei, K. A., Steidel, C. C., & Siana, B. 2013, *ApJ*, 765, 47,  
doi: [10.1088/0004-637X/765/1/47](https://doi.org/10.1088/0004-637X/765/1/47)
- Nonino, M., Dickinson, M., Rosati, P., et al. 2009, *ApJS*, 183, 244, doi: [10.1088/0067-0049/183/2/244](https://doi.org/10.1088/0067-0049/183/2/244)
- Oesch, P. A., Montes, M., Reddy, N., et al. 2018, *ApJS*, 237, 12, doi: [10.3847/1538-4365/aacb30](https://doi.org/10.3847/1538-4365/aacb30)
- Oesch, P. A., Brammer, G., Naidu, R. P., et al. 2023, *MNRAS*, 525, 2864, doi: [10.1093/mnras/stad2411](https://doi.org/10.1093/mnras/stad2411)
- Ouchi, M., Mobasher, B., Shimasaku, K., et al. 2009, *ApJ*, 706, 1136, doi: [10.1088/0004-637X/706/2/1136](https://doi.org/10.1088/0004-637X/706/2/1136)
- Pahl, A. J., Shapley, A., Steidel, C. C., et al. 2023, *MNRAS*, 521, 3247, doi: [10.1093/mnras/stad774](https://doi.org/10.1093/mnras/stad774)
- Planck Collaboration, Adam, R., Aghanim, N., et al. 2016, *A&A*, 596, A108, doi: [10.1051/0004-6361/201628897](https://doi.org/10.1051/0004-6361/201628897)
- Popesso, P., Concas, A., Cresci, G., et al. 2023, *MNRAS*, 519, 1526, doi: [10.1093/mnras/stac3214](https://doi.org/10.1093/mnras/stac3214)
- Rafelski, M., Teplitz, H. I., Gardner, J. P., et al. 2015, *AJ*, 150, 31, doi: [10.1088/0004-6256/150/1/31](https://doi.org/10.1088/0004-6256/150/1/31)
- Rauch, M., Becker, G. D., Haehnelt, M. G., et al. 2011, *MNRAS*, 418, 1115,  
doi: [10.1111/j.1365-2966.2011.19556.x](https://doi.org/10.1111/j.1365-2966.2011.19556.x)
- Rieke, M. J., Robertson, B., Tacchella, S., et al. 2023, *ApJS*, 269, 16, doi: [10.3847/1538-4365/acf44d](https://doi.org/10.3847/1538-4365/acf44d)
- Rieke, Marcia, Robertson, Brant, Tacchella, Sandro, et al. 2023, Data from the JWST Advanced Deep Extragalactic Survey (JADES), STScI/MAST,  
doi: [10.17909/8TDJ-8N28](https://doi.org/10.17909/8TDJ-8N28)
- Rivera-Thorsen, T. E., Hayes, M., & Melinder, J. 2022, *arXiv e-prints*, arXiv:2206.10799,  
<https://arxiv.org/abs/2206.10799>
- Robertson, B. E., Ellis, R. S., Furlanetto, S. R., & Dunlop, J. S. 2015, *ApJL*, 802, L19,  
doi: [10.1088/2041-8205/802/2/L19](https://doi.org/10.1088/2041-8205/802/2/L19)
- Robertson, B. E., Furlanetto, S. R., Schneider, E., et al. 2013, *ApJ*, 768, 71, doi: [10.1088/0004-637X/768/1/71](https://doi.org/10.1088/0004-637X/768/1/71)
- Salpeter, E. E. 1955, *ApJ*, 121, 161, doi: [10.1086/145971](https://doi.org/10.1086/145971)
- Santini, P., Fontana, A., Grazian, A., et al. 2009, *A&A*, 504, 751, doi: [10.1051/0004-6361/200811434](https://doi.org/10.1051/0004-6361/200811434)
- Santini, P., Fontana, A., Castellano, M., et al. 2017, *ApJ*, 847, 76, doi: [10.3847/1538-4357/aa8874](https://doi.org/10.3847/1538-4357/aa8874)
- Saxena, A., Pentericci, L., Ellis, R. S., et al. 2022, *MNRAS*, 511, 120, doi: [10.1093/mnras/stab3728](https://doi.org/10.1093/mnras/stab3728)
- Seaton, M. J. 1979, *MNRAS*, 187, 73,  
doi: [10.1093/mnras/187.1.73P](https://doi.org/10.1093/mnras/187.1.73P)
- Shapley, A. E., Steidel, C. C., Pettini, M., Adelberger, K. L., & Erb, D. K. 2006, *ApJ*, 651, 688,  
doi: [10.1086/507511](https://doi.org/10.1086/507511)
- Shapley, A. E., Steidel, C. C., Strom, A. L., et al. 2016, *ApJL*, 826, L24, doi: [10.3847/2041-8205/826/2/L24](https://doi.org/10.3847/2041-8205/826/2/L24)
- Shen, X., Hopkins, P. F., Faucher-Giguère, C.-A., et al. 2020, *MNRAS*, 495, 3252, doi: [10.1093/mnras/staa1381](https://doi.org/10.1093/mnras/staa1381)
- Skelton, R. E., Whitaker, K. E., Momcheva, I. G., et al. 2014, *ApJS*, 214, 24, doi: [10.1088/0067-0049/214/2/24](https://doi.org/10.1088/0067-0049/214/2/24)
- Speagle, J. S., Steinhardt, C. L., Capak, P. L., & Silverman, J. D. 2014, *ApJS*, 214, 15,  
doi: [10.1088/0067-0049/214/2/15](https://doi.org/10.1088/0067-0049/214/2/15)
- Steidel, C. C., Bogosavljević, M., Shapley, A. E., et al. 2018, *ApJ*, 869, 123, doi: [10.3847/1538-4357/aaed28](https://doi.org/10.3847/1538-4357/aaed28)
- Steidel, C. C., Pettini, M., & Adelberger, K. L. 2001, *ApJ*, 546, 665, doi: [10.1086/318323](https://doi.org/10.1086/318323)

- Teplitz, H. I., Rafelski, M., Kurczynski, P., et al. 2013, *AJ*, 146, 159, doi: [10.1088/0004-6256/146/6/159](https://doi.org/10.1088/0004-6256/146/6/159)
- Vanzella, E., Guo, Y., Giavalisco, M., et al. 2012, *ApJ*, 751, 70, doi: [10.1088/0004-637X/751/1/70](https://doi.org/10.1088/0004-637X/751/1/70)
- Vanzella, E., de Barros, S., Castellano, M., et al. 2015, *A&A*, 576, A116, doi: [10.1051/0004-6361/201525651](https://doi.org/10.1051/0004-6361/201525651)
- Vanzella, E., de Barros, S., Vasei, K., et al. 2016, *ApJ*, 825, 41, doi: [10.3847/0004-637X/825/1/41](https://doi.org/10.3847/0004-637X/825/1/41)
- Vanzella, E., Nonino, M., Cupani, G., et al. 2018, *MNRAS*, 476, L15, doi: [10.1093/mnras/sly023](https://doi.org/10.1093/mnras/sly023)
- Wang, X., Teplitz, H. I., Smith, B. M., et al. 2023, arXiv e-prints, arXiv:2308.09064, doi: [10.48550/arXiv.2308.09064](https://doi.org/10.48550/arXiv.2308.09064)
- Williams, C. C., Tacchella, S., Maseda, M. V., et al. 2023, *ApJS*, 268, 64, doi: [10.3847/1538-4365/acf130](https://doi.org/10.3847/1538-4365/acf130)
- Williams, Christina, Tacchella, Sandro, & Maseda, Michael. 2023, Data from the JWST Extragalactic Medium-band Survey (JEMS), STScI/MAST, doi: [10.17909/FSC4-DT61](https://doi.org/10.17909/FSC4-DT61)
- Yuan, F.-T., Argudo-Fernández, M., Shen, S., et al. 2018, *A&A*, 613, A13, doi: [10.1051/0004-6361/201731865](https://doi.org/10.1051/0004-6361/201731865)
- Yuan, F.-T., Burgarella, D., Corre, D., et al. 2019, *A&A*, 631, A123, doi: [10.1051/0004-6361/201935975](https://doi.org/10.1051/0004-6361/201935975)
- Yuan, F.-T., Zheng, Z.-Y., Lin, R., Zhu, S., & Rahna, P. T. 2021, *ApJL*, 923, L28, doi: [10.3847/2041-8213/ac4170](https://doi.org/10.3847/2041-8213/ac4170)
- Zackrisson, E., Inoue, A. K., & Jensen, H. 2013, *ApJ*, 777, 39, doi: [10.1088/0004-637X/777/1/39](https://doi.org/10.1088/0004-637X/777/1/39)
- Zhan, H. 2018, in 42nd COSPAR Scientific Assembly, Vol. 42, E1.16–4–18